35th EPS Conference on Plasma Phys. Hersonissos, 9 - 13 June 2008 ECA Vol.**32D**, P-4.064 (2008)

Modelling observations of mode polarisation from MAST

R G L Vann[1], L Appel[2], P J Denner[1], M P Gryaznevich[2], M K Lilley[3], R Martin[2], S D Pinches[2], S E Sharapov[2], C T N Willis[1] and the MAST team

[1] *Department of Physics, University of York, Heslington, York YO10 5DD, UK*

[2] *Euratom/UKAEA Fusion Association, Culham Science Centre, Abingdon, Oxfordshire OX14 3DB, UK*

[3] *Department of Physics, Imperial College of Science, Technology & Medicine, Exhibition Road, London SW7 2AZ, UK*

Superthermal energetic particles (EPs) play an important role in the plasmas of magnetically-confined nuclear fusion experiments [1]. Sources of EPs include neutral beam injection (NBI) heating, ion cyclotron resonance heating (ICRH) and fusion-produced alpha-particles. It is critical to the success of any future fusion reactor both that the kinetic energy of these EPs is contained within the plasma sufficiently long to sustain the fusion process and also that the presence of these particles does not destabilize the plasma. Alfvénic eigenmodes are of particular interest as an example of collective instabilities that may be resonantly excited by EPs [2, 3]. In this paper we categorize magnetic activity on the Mega-Amp Spherical Tokamak (MAST) [4] by direct measurement of the orientation, polarisation and handedness of the magnetic perturbation. We calculate these quantities by combining the signals from a Mirnov probe which contains three concentric coils oriented radially, vertically and toroidally (denoted below by subscripts r, z and ϕ, respectively). These probes are mounted sufficiently far from the wall that they can measure the radial field, and are therefore an advance on previous orientation measurements made on NSTX [5]. We take the Hanning-windowed Fourier transform of the perturbed magnetic field time signals to obtain

$$\delta\mathbf{B} \;=\; \sum_{j\in\{r,z,\phi\}} \hat{\mathbf{e}}_j \delta B_j \cos\left(\omega t + \theta_j\right) \tag{1}$$

where the $\{\delta B_j \geq 0\}$. $\delta\mathbf{B}$ traces out an ellipse and can be written

$$\delta\mathbf{B} = \delta\mathbf{B}_{\text{major}} \cos(\omega t + \psi) + \delta\mathbf{B}_{\text{minor}} \sin(\omega t + \psi) \tag{2}$$

where

$$\cos(2\psi) = \sum_{j\in\{r,z,\phi\}} \delta B_j^2 \cos 2\theta_j \qquad \sin(2\psi) = \sum_{j\in\{r,z,\phi\}} \delta B_j^2 \sin 2\theta_j. \tag{3}$$

The vectors $\delta\mathbf{B}_{\text{major}}$ and $\delta\mathbf{B}_{\text{minor}}$ are the major and minor axes, respectively, of the ellipse traced out by $\delta\mathbf{B}$. It is important to recognise that $\delta\mathbf{B}_{\text{major}}$ and $\delta\mathbf{B}_{\text{minor}}$ are not themselves basis vectors but are composed of the basis vectors $\delta B_j \mathbf{e}_j$. Two scalar measures of the mode orientation are the angles between the equilibrium field $\mathbf{B}_0$ and the major

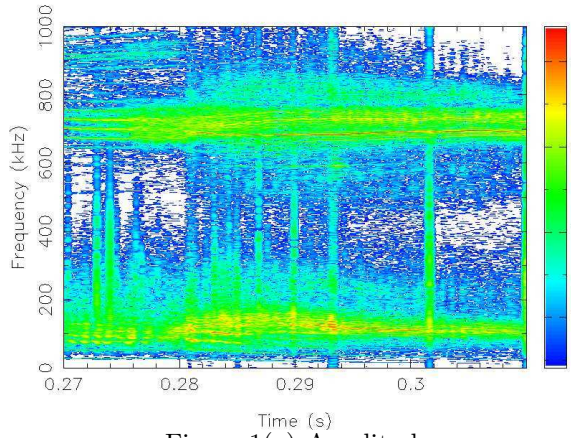

Figure 1(a) Amplitude

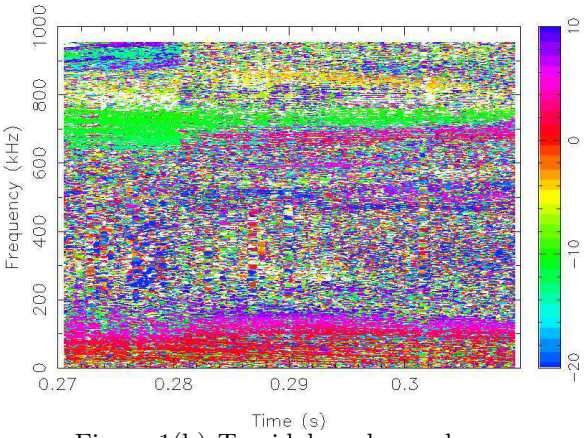

Figure 1(b) Toroidal mode number n

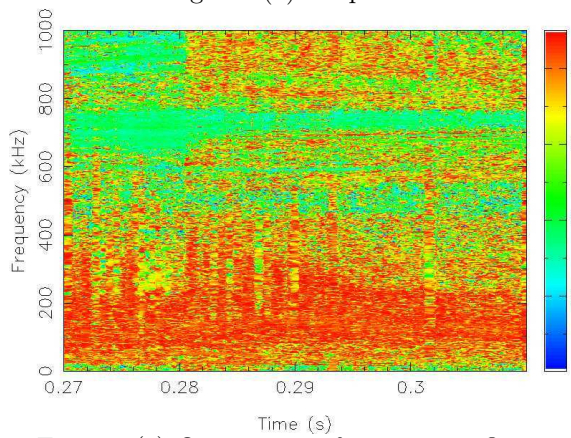

Figure 1(c) Orientation of major axis Θ_{major}

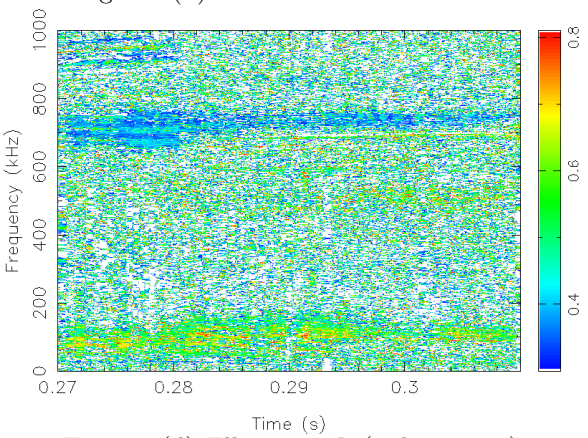

Figure 1(d) Ellipticity $\mathcal{R}$ (polarisation)

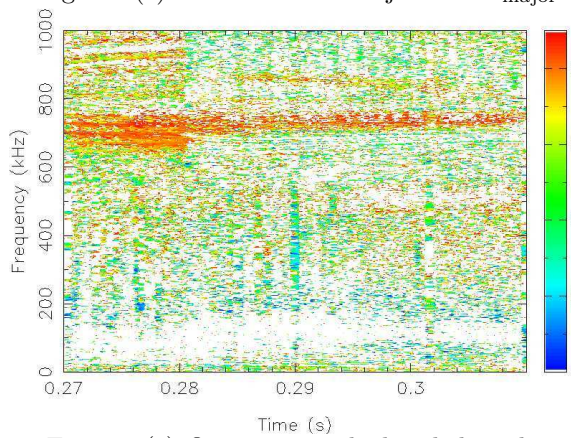

Figure 1(e) $\Theta_{\text{H}} < 90°$: right-handed modes

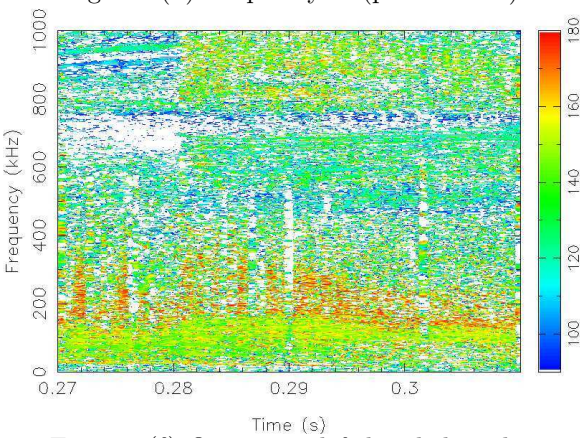

Figure 1(f) $\Theta_{\text{H}} > 90°$: left-handed modes

Figure 1: Experimental observation of Alfvénic activity in NBI-heated MAST shot 18690. This analysis (see text for details) suggests that the waves at $\omega/2\pi \sim 110$kHz are toroidicity-induced Alfvén eigenmodes (TAEs) and the waves at $\omega/2\pi \sim 700$kHz are compressional Alfvén eigenmodes (CAEs) (corresponding to shear and fast magnetoacoustic waves, respectively).

and minor axes, denoted by Θ_{major} and Θ_{minor}, respectively. The polarisation is given by $\mathcal{R} = |\delta\mathbf{B}_{\text{minor}}|/|\delta\mathbf{B}_{\text{major}}|$: $\mathcal{R} = 0$ implies plane polarisation; $\mathcal{R} = 1$ implies circular polarisation. Furthermore, let us define Θ_{H} as the angle between $\delta\mathbf{B}_{\text{major}} \times \delta\mathbf{B}_{\text{minor}}$ and $\mathbf{B}_0$ (i.e. $\Theta_{\text{H}} = \arccos\left((\delta\mathbf{B}_{\text{major}} \times \delta\mathbf{B}_{\text{minor}}) \,.\, \mathbf{B}_0/|\delta\mathbf{B}_{\text{major}}|\,|\delta\mathbf{B}_{\text{minor}}|\,|\mathbf{B}_0|\right)$. Since the minor axis is

realised a quarter period after the major axis, $\Theta_H < 90°$ implies that the perturbation is right-handed with respect to $\mathbf{B}_0$; $\Theta_H > 90°$ implies that the perturbation is left-handed. Additionally we calculate the toroidal mode number n using coils at equivalent poloidal locations and distinct toroidal locations.

To characterize modes on MAST [4] we use signals from the "OMAHA" Mirnov array, capable of sampling at 10MHz and situated 20cm above the midplane at a major radius of 1.7m. Five vertically-oriented coils at relative toroidal locations $\{0°, 13°, 27°, 45°, 79°\}$ are used for calculating the toroidal mode number. The equilibrium field $\mathbf{B}_0$ is calculated using the EFIT equilibrium reconstruction code [6]. In this paper we study NBI-heated MAST shot 18690 in the time range 0.27-0.31s. The data are displayed in Figure 1 – the subplots show quantities as functions of time and frequency. Subplot (a) shows the amplitude on a logarithmic scale: there are two families of modes: one at $\sim$ 110kHz and one at $\sim$ 700kHz. Subplot (b) shows the toroidal mode numbers: the lower frequency modes have $0 < n < 5$; the higher frequency modes have negative toroidal mode number. Subplot (c) shows the angle between the major axis of the perturbation and the equilibrium field. The lower frequency modes are oriented approximately perpendicular to the equilibrium field and the higher frequency modes are oriented quasi-parallel. The orientation of the minor axis has not been plotted; it is quasi-perpendicular for both sets of modes. Subplot (d) shows the polarisation of the modes: the lower frequency modes are more circularly polarised. Subplots (e) and (f) isolate left- and right-handed perturbations, respectively. The higher frequency modes are right-handed with respect to the equilibrium field, whilst the lower frequency modes are left-handed. (I.e. the higher (lower) frequency modes rotate (anti-)clockwise about the equilibrium field.) On the basis of this analysis, these lower and higher frequency modes are identified as being toroidicity-induced Alfvén eigenmodes (TAEs) and compressional Alfvén eigenmodes (CAEs), respectively.

We notice in the amplitude plot a strong signal from 0.28s with frequency 690kHz that follows the statistics of the lower frequency modes rather than the other higher frequency modes – it is quasi-perpendicular, circularly polarised, left handed and it has positive toroidal mode number. It cannot be a toroidicity-induced (poloidal mode number m coupling to $m+1$) mode since its frequency is too high, but it shares the characteristics of a shear wave. We therefore identify it as a higher gap mode: either an ellipticity (m coupling to $m+2$) or triangularity (m coupling to $m+3$) induced mode. We note that this wave cannot be distinguished from the compressional wave by looking only at the wave's frequency.

We have performed the analysis described above for a large number of MAST shots and have found that the characteristics discussed above are general, rather than specific to this particular shot and time window. The resulting statistics are shown in Table 1. The first row catalogues the relatively low frequency mode while the second row cata-

Mode	Θ_1	Θ_2	$\omega/2\pi$ (kHz)	Ellipticity $\mathcal{R}$	Mode number n	Handedness
TAE	$\gtrsim 60°$	$\gtrsim 60°$	(60, 150)	(0.4, 0.8)	$0 < n \lesssim 8$	Left
CAE	$\lesssim 40°$	$\gtrsim 60°$	$\gtrsim 150$	(0.2, 0.5)	$-20 \lesssim n \lesssim -5$	Right

Table 1: Characteristics of candidate TAEs and CAEs from a number of observations from MAST. The two types of mode can be distinguished without referring to their frequency. This is crucial when differentiating between a CAE and a higher-gap shear mode such as an ellipticity or triangularity induced eigenmode (EAE or NAE).

logues the relatively high frequency mode.

A key question is to what extent the local measurements made at the probe reflect the wave properties at the mode location within the plasma. To tackle this question we have begun theoretical modelling using the equilibrium codes EFIT [6] and HELENA [7], and the eigenfunction code CASTOR [8]. The Alfvén continuum may be plotted as the location of discontinuities in computed eigenfunctions. In principle, the eigenfunctions can be compared directly with what is measured in experiment. However, before this can be done, the following challenges have to be overcome: (i) our current use of straight field line coordinates causes problems at the separatrix; how much does it affect the eigenfunction if only plasma up to normalised $\psi = 90\%$, say, is considered? (ii) the spectrum at the edge is strongly dependent on the pedestal profile, (iii) calculating the remnant of the wavefunction that tunnels through the continuum is difficult (iv) MHD breaks down as the cyclotron frequency is approached, so a more sophisticated treatment [9] is needed.

This work was partly funded by the UK EPSRC, the Nuffield Foundation and the European Communities under the Contract of Association between EURATOM and UKAEA. The views and opinions expressed herein do not necessarily reflect those of the European Commission.

[1] S. D. Pinches *et al.*, *Plasma Physics and Controlled Fusion* **46** B187 (2004)

[2] W. W. Heidbrink, *Phys. Plasmas* **15** 055501 (2008)

[3] L. Appel *et al.*, "Compressional Alfvén eigenmodes on MAST" submitted to *Plasma Physics Control. Fusion* (2008)

[4] A. Sykes *et al.*, *Nucl. Fusion* **41** 1423 (2001)

[5] N. N. Gorelenkov, E. D. Fredrickson, W. W. Heidbrink, N. A. Crocker, S. Kubota and W. A. Peebles, *Nucl. Fusion* **46** S933 (2006)

[6] L. L. Lao, H. E. St John, R. D. Stambaugh, A. G. Kellman and W. Pfeiffer, *Nucl. Fusion* **25** 1611 (1985)

[7] G. T. A. Huysmans, J. P. Goedbloed and W. Kerner *CP90 Conf. on Comp. Physics* (Singapore: Word Scientific) p371 (1991)

[8] W. Kerner, J. P. Goedbloed, G. T. A. Huysmans, S. Poedts and E. Schwarz, *J. Comp. Phys.* **142** 271 (1998)

[9] M. K. Lilley and S. E. Sharapov, *Proc. 35th EPS Conference on Plasma Physics, Crete* (2008)